2000-010 CONF 331

2 March 2000

Search for charginos and neutralinos in e^+e^- interactions at $\sqrt{s} = 192$–196–200–202 GeV

DELPHI Collaboration

PRELIMINARY RESULTS

T.Alderweireld [1], P. Andersson [2], M.Espirito Santo[3]
I.Gil [4],K. Hultqvist[2], A.Lipniacka[2],
M.Margoni [5], F.Mazzucato[5], P.Rebecchi[3]

[1] IISN, U. Mons Hainaut, Place du Parc, 7000 Mons, Belgium
[2] Fysikum, Stockholm University, Box 6730, S-11385 Stockholm, Sweden
[3] CERN, CH-1211 Geneva 23, Switzerland
[4] IFIC, Valencia-CSIC and DFAMN, U. de Valencia, E-46100 Burjassot (Valencia), Spain
[5] I.N.F.N. sezione di Padova, Padova, Italy

Abstract

An update of the searches for charginos, neutralinos and gravitinos is presented, based on a data sample corresponding to the 227 pb^{-1} recorded by the DELPHI detector in 1999, at centre-of-mass energies of 192, 196, 200 and 202 GeV. No evidence for a signal was found. The lower chargino mass limits are 5-6 GeV/c^2 higher than those obtained at a centre-of-mass energy of 189 GeV. The (μ,M_2) MSSM domain excluded by combining the chargino searches with neutralino searches at the Z resonance implies a limit on the mass of the lightest neutralino which, for a heavy sneutrino, is constrained to be above 35.2 GeV/c^2 for $\tan\beta \geq 1$. Upper limit at 95 % CL on the neutralino production cross–section times branching fraction are derived.

(Results for the $XXXV^{th}$ Moriond conference)

1 Introduction

In 1999, the LEP centre–of–mass energy reached 192, 196, 200 and 202 GeV, and the DELPHI experiment collected an integrated luminosity of 227 pb^{-1}. These data have been analysed to search for charginos and neutralinos, supersymmetric partners of Higgs and gauge bosons, predicted by supersymmetric (SUSY) models [1].

A description of the parts of the DELPHI detector relevant to the present paper can be found in [2], while a complete description is given in [3].

The conservation of R-parity, implying a stable lightest supersymmetric particle (LSP), is assumed. This also means that charginos and neutralinos are pair produced in e^+e^- collisions. The analysis was performed in the framework of the Minimal Supersymmetric extension of the Standard Model (MSSM), with universal parameters at the high mass scale typical of Grand Unified Theories (GUT's) [1]. The parameters of this model relevant to the present searches are the masses M_1 and M_2 of the gaugino sector (which are assumed to satisfy the GUT relation $M_1 = \frac{5}{3}\tan^2\theta_W M_2 \approx 0.5 M_2$ at the electroweak scale), the universal mass m_0 of the scalar fermion sector, the Higgs mass parameter μ, and the ratio $\tan\beta$ of the vacuum expectation values of the two Higgs doublets. In this paper it is assumed that m_0 =1 TeV. Scalar mass unification is assumed, except in the chargino search where the sneutrino mass is considered to be a free parameter.

As in Ref. [2] for the chargino search both cases where either the lightest neutralino ($\tilde{\chi}_1^0$) or the gravitino ($\tilde{G}$) is the LSP are considered. In the former case, the decay of the chargino is $\tilde{\chi}_1^\pm \to \tilde{\chi}_1^0 f\bar{f}'$ ($f\bar{f}'$ can be quarks or leptons) and the events are characterised by missing energy carried by the escaping $\tilde{\chi}_1^0$. In some areas of the parameter space, the charginos can decay to heavier neutralinos giving rise to a cascade effect: $\tilde{\chi}_1^\pm \to \tilde{\chi}_2^0 f_1\bar{f}_1' \to \tilde{\chi}_1^0 f_1\bar{f}_1' f_2\bar{f}_2$ ($f_1\bar{f}_1' f_2\bar{f}_2$ can be quarks or leptons). The decay $\tilde{\chi}_2^0 \to \tilde{\chi}_1^0\gamma$ may occur for small $\mu \approx -M_2$. So the following decay channels were defined:

- The *leptonic* channel ($\ell\ell$): the decay products are only leptons and the LSPs.
- The *hadronic* channel (*jets*): the decay products are only quarks and the LSPs.
- The *semi-leptonic* channel ($jj\ell$): the decay products are quarks, leptons and the LSPs.
- The *radiative* channel (*rad*): there is at least one isolated photon among the decay products.

In the neutralino search the lightest neutralino ($\tilde{\chi}_1^0$) was always assumed to be the LSP. Two neutralino pair production processes have been considered, $\tilde{\chi}_1^0\tilde{\chi}_2^0$ and $\tilde{\chi}_1^0\tilde{\chi}_3^0$. The decay of the neutralinos is $\tilde{\chi}_i^0 \to \tilde{\chi}_1^0 f\bar{f}$ ($f\bar{f}$ can be quarks or leptons and i=2,3) and the events are characterised by missing energy carried by the escaping $\tilde{\chi}_1^0$. So the following decay channels were defined:

- The *electron* channel (ee): the decay products are only electrons and the LSP.
- The *muon* channel (mm): the decay products are only muons and the LSP.
- The *hadronic* channel (qq): the decay products are only quarks and the LSP.

In this scenario the likelihood ratio method [4] was used to optimize the search for charginos and neutralinos. An overview of this method and details of the implementation are given in 3.1. The method applied for this present chargino analysis is the same used at centre–of–mass energy of 189 GeV [8]. For the neutralino for the first time a similar likelihood ratio approach is used.

If the gravitino is the LSP, the decay $\tilde{\chi}_1^0 \to \tilde{G}\gamma$ is possible [5–7]. If the gravitino is sufficiently light (with a mass below about 10 eV/c^2 [7]), this decay takes place within the detector. As gravitinos escape detection, the typical signature of these SUSY events

is missing energy and isolated photons. The selection criteria already used at a centre–of–mass energy of 183 GeV are applied in this scenario. The detailed description of the analysis can be found in Ref. [2].

2 Data samples and event generators

To evaluate the signal efficiencies and background contaminations, events were generated using several different programs. All relied on `JETSET` 7.4 [9], tuned to LEP 1 data [10], for quark fragmentation.

The program `SUSYGEN` [11] was used to generate events with chargino production and decay in both the neutralino LSP and the gravitino LSP scenarios, and to calculate masses, cross-sections and branching ratios for each adopted parameter set. `SUSYGEN` was used to generate neutralino production and decays. These agree with the calculations of Ref. [12]. Details of the signal samples generated are given in section 4.

The background process $e^+e^- \to q\bar{q}(n\gamma)$ was generated with `PYTHIA 5.7` for 192 GeV data and `PYTHIA 6.1` for the other energies [9], while `DYMU3` [13] and `KORALZ 4.2` [14] were used for $\mu^+\mu^-(\gamma)$ and $\tau^+\tau^-(\gamma)$, respectively. The generator of Ref. [15] was used for $e^+e^- \to e^+e^-$ events. Processes leading to four-fermion final states, $(Z/\gamma)^*(Z/\gamma)^*$, W^+W^-, $We\nu_e$ and Ze^+e^-, were generated using `EXCALIBUR` [16] and `GRC4F` [17].

Two-photon interactions leading to hadronic final states were generated using `TWOGAM` [18], including the VDM (Vector Dominance Model), QCD and QPM components. The generators of Berends, Daverveldt and Kleiss [19] were used for leptonic final states.

The generated signal and background events were passed through the detailed simulation of the DELPHI detector [3] and then processed with the same reconstruction and analysis programs as real data events. The number of simulated events from different background processes was several times (a factor varying from 2 to 140 depending on the background process) the number of real events recorded.

3 Event selections

The criteria used to select events were defined on the basis of the simulated signal and background events. The selections for charged and neutral particles were similar to those presented in [8], requiring charged particles to have momentum above 100 MeV/c and to extrapolate back to within 5 cm of the main vertex in the transverse plane, and to within twice this distance in the longitudinal direction. Calorimeter energy clusters above 100 MeV were taken as neutral particles if not associated to any charged particle track. The particle selection was followed by different event selections for the different signal topologies considered in the application of the likelihood ratio method. The detailed description of the analysis done in the unstable $\tilde{\chi}_1^0$ case can be found in Ref. [2]. Neutralino events were selected if they had at least two charged tracks, transverse momentum greater than 4 GeV and if $|cos(\theta_{miss})|$ was less than 0.998 .

3.1 The likelihood ratio method

In the likelihood ratio method used, several discriminating variables are combined into one on the basis of their one-dimensional probability density functions (pdf). If the variables used are independent, this gives the best possible background suppression

for a given signal efficiency [4]. For a set of variables $\{x_i\}$, the pdf's of these variables are estimated by normalised frequency distributions for the signal and the background samples. We denote the pdf's of these variables $f_i^S(x_i)$ for the signal events and $f_i^B(x_i)$ for the background events submitted to the same selection criteria. The likelihood ratio function is defined as $\mathcal{L}_\mathcal{R} = \prod_{i=1}^{n} \frac{f_i^S(x_i)}{f_i^B(x_i)}$. Events with $\mathcal{L}_\mathcal{R} > \mathcal{L}_{\mathcal{R}_{CUT}}$ are selected as candidate signal events. The optimal set of variables and the value of $\mathcal{L}_{\mathcal{R}_{CUT}}$ were defined in order to minimise the excluded cross-section expected in the absence of a signal (at 95% confidence level). The variables $\{x_i\}$ used to build the $\mathcal{L}_\mathcal{R}$ functions in the present chargino analysis were [8]: the visible energy ($E_{\rm vis}$), visible mass ($M_{\rm vis}$), missing transverse momentum ($p_T^{\rm miss}$), polar angle of the missing momentum, number of charged particles, total number of particles, acoplanarity, acollinearity, ratio of electromagnetic energy to total energy, percentage of total energy within 30° of the beam axis, kinematic information concerning the isolated photons, leptons and two most energetic charged particles and finally the jet characteristics.

The variables $\{x_i\}$ used to build the $\mathcal{L}_\mathcal{R}$ functions in the present neutralino analysis were: the S' variable [20], visible energy ($E_{\rm vis}$), electromagnetic energy, hadronic energy, maximum energy of a neutral particle, percentage of total energy within 40° of the beam axis, ratio between the maximum energy of a charged particle and the visible energy, number of charged tracks, maximum track momentum and transverse momentum, transverse missing momentum normalized to the beam energy, ratio between the missing momentum and the visible energy, sum of the absolute values of the momenta in the transverse plane w.r.t the beam and in the plane transverse to the thrust axis, invariant mass, missing mass, missing mass w.r.t the jet direction, missing transverse mass, missing longitudinal energy, scaled acoplanarity, aplanarity, missing momentum polar angle, angle between the two jets, angle between each jet and the missing momentum direction, event and jet thrust, event and jet sphericity, thrust and sphericity computed versus the missing momentum direction and finally the minimum *ycut* value to cluster an event in two jets using the Durham algorithm [21].

3.2 Chargino analysis

The signal and background events were divided into four mutually exclusive topologies:

- The $\ell\ell$ topology with no more than five charged particles and no isolated photons.
- The $jj\ell$ topology with more than five charged particles and at least one isolated lepton and no isolated photons.
- The *jets* topology with more than five charged particles and no isolated photons or leptons.
- The *rad* topology with at least one isolated photon.

The events in a given topology are mostly events of the corresponding decay channel, but events from other channels may also contribute. For instance, for low mass difference, ΔM, between the chargino and the lightest neutralino (and thus low visible energy) some events with hadronic decays are selected in the leptonic topology, and some mixed decay events with the isolated lepton unidentified enter into the hadronic topology. This migration effect tends to disappear as ΔM increases. This effect was taken into account in the final efficiency and limit computations.

The properties of the chargino decay products are mainly governed by the ΔM value. For low ΔM, the signal events are similar to $\gamma\gamma$ events, for high ΔM to four-fermion final

states (W^+W^-, ZZ,..) while for intermediate ΔM values, the background is composed of many SM processes in comparable proportions.

The signal events were simulated for 104 combinations of $\tilde{\chi}_1^\pm$ and $\tilde{\chi}_1^0$ masses for seven chargino mass values ($M_{\tilde{\chi}_1^\pm} \approx$ 100, 98, 94, 85, 70, 50 and 45 GeV/c^2) and with ΔM ranging from 3 GeV/c^2 to 80 GeV/c^2. A total of 208000 chargino events (2000 per combination) was generated and passed through the complete simulation of the DELPHI detector. The kinematic properties (acoplanarity, $E_{\rm vis}$, $p_T^{\rm miss}$,..) of the signal events were studied in terms of their mean value and standard deviation, and six ΔM regions were defined in order to have signal events with similar properties (table 1).

In each of these 24 windows (four topologies, six ΔM regions), a likelihood ratio function was defined. The generation of these 24 functions was performed in five steps:

- The signal distributions of all the variables used in this analysis (see section 3.1) were built with signal events generated with parameter sets giving rise to charginos and neutralinos with masses in the corresponding ΔM region. For each ΔM region the events were classified according to the above topological cuts. The background distributions were built with background events passing the same topological cuts.
- Different preselection cuts, for each ΔM region, were applied in order to reduce the high cross-section backgrounds (two-photon interactions and Bhabha events) and to generate the pdf's. The pdf's were then generated as mentioned in 3.1.
- Then, to reduce statistical fluctuations a smoothing was performed by passing the 24 sets of pdf's for signal and background through a triangular filter [22].
- In each window all the combinations of the pdf's were tested, starting from a minimal set of four variables. Every combination defined a $\mathcal{L}_\mathcal{R}$ function (see section 3.1) and a $\mathcal{L}_{\mathcal{R}cut}$ computed in order to have the minimal expected excluded cross-section at 95% C.L. using the monochannel Bayesian formula [23]. The parameters entering this computation were the number of expected background events and the efficiency of the chargino selection. The efficiency of the chargino selection was defined in this case, as the number of events satisfying $\mathcal{L}_\mathcal{R} > \mathcal{L}_{\mathcal{R}cut}$ divided by the total number of chargino events satisfying the topological cuts.
- The combination of variables corresponding to the lowest excluded cross-section defined the $\mathcal{L}_\mathcal{R}$ function and the $\mathcal{L}_{\mathcal{R}cut}$ of this window.

Finally, the selection to be applied for SUSY models with ΔM inside one such window was defined as a logical OR of the criteria for several windows, chosen to minimise the excluded cross-section expected in the absence of a signal [8].

These five steps were applied for each centre–of–mass energies producing 96 windows of investigation.

	ΔM regions
1	$3 \leq \Delta M < 5$ GeV/c^2
2	$5 \leq \Delta M < 10$ GeV/c^2
3	$10 \leq \Delta M < 25$ GeV/c^2
4	$25 \leq \Delta M < 35$ GeV/c^2
5	$35 \leq \Delta M < 50$ GeV/c^2
6	50 GeV/$c^2 \leq \Delta M$

Table 1: Definitions of the ΔM regions for the charginos search.

3.3 Neutralino analysis

The first stage of the analysis was to remove the most dominant SM background processes, therefore events were selected if:

1. The polar angle of the most energetic electro-magnetic cluster was above 5 degrees.
2. The energy in a 30 degrees cone around the beam axis was less than 80% of the total visible energy.
3. The sum of the moduli of all particle momenta was greater than 30 GeV or the polar angle of the missing momentum was above 20 degrees.
4. acoplanarity and acollinearity greater than 5 degrees.
5. The total electromagnetic energy was less than 60% of the centre–of–mass energy.
6. The most energetic electromagnetic cluster was less than 40% of the centre–of–mass energy.
7. The acoplanarity was greater than 20 degrees or the effective centre–of–mass energy outside the range 80-110 GeV.
8. No signal was detected in any isolated hermeticity tagger.
9. The most energetic photon had an energy below 50 GeV.
10. The sum of the visible energy and the total transverse momentum w.r.t. the thrust axis had to be less than 165 GeV.

The first criteria rejects off-momentum electrons deriving from beam-gas interactions. The second and third cuts reject the bulk of two-photon processes. The fourth to the sixth requirements are aimed to cut Bhabha and non radiative two fermion events. The bulk of the remaining two fermion processes are rejected by the seventh to the nineth criteria. The last cut is against four fermion processes. After this preselection the signal and background events were divided into three mutually exclusive topologies:

- The ee topology with only two charged particles, both identified as electrons
- The mm topology with only two charged particles, both identified as muons
- The qq topology with more than five charged particles and no isolated photons or leptons.

The properties of the neutralino decay products are mainly governed by the ΔM value, here defined as the mass difference between the produced neutralino of highest order ($\tilde{\chi}^0_2$ or $\tilde{\chi}^0_3$) and the LSP ($\tilde{\chi}^0_1$). For low ΔM, the signal events are similar to $\gamma\gamma$ events, for high ΔM to four-fermion final states (W^+W^-, ZZ,..) while for intermediate ΔM values, the background is composed of manly of two-fermion processes.

The signal events were simulated for 77 combinations of $\tilde{\chi}^0_1$ and $\tilde{\chi}^0_2$ masses for all neutralino topologies. A total of 231000 neutralino events was generated and passed through the complete simulation of the DELPHI detector. The kinematic properties (acoplanarity, $E_{\rm vis}$, $p_T^{\rm miss}$,..) of the signal events were studied in terms of their mean value and standard deviation, and five ΔM regions were defined in order to have signal events with similar properties (table 1).

In each of these 15 windows (three topologies, five ΔM regions), a likelihood ratio function was defined. For each variable, the one-dimensional probability density function (pdf) was computed with a similar procedure to what described for chargino analysis. In this analysis the likelihood ratio function is defined as $\mathcal{L}_{\mathcal{R}} = \prod_{i=1}^{n} \frac{f_i^B(x_i)}{f_i^B(x_i)+f_i^S(x_i)}$. This definition gives likelihood ratio values between 0 and 1 with the signal (background) events peaked in the low (high) value region. Events with $\mathcal{L}_{\mathcal{R}} < \mathcal{L}_{\mathcal{R}_{CUT}}$ are selected as candidate signal events. As in the chargino analysis, the optimal set of variables and the

value of $\mathcal{L}_{\mathcal{R}cut}$ were defined in order to minimise the excluded cross-section expected in the absence of a signal (at 95% confidence level).

	ΔM regions
1	$5 \leq \Delta M < 10$ GeV/c^2
2	$10 \leq \Delta M < 25$ GeV/c^2
3	$25 \leq \Delta M < 40$ GeV/c^2
4	$40 \leq \Delta M < 60$ GeV/c^2
5	60 GeV/$c^2 \leq \Delta M$

Table 2: Definitions of the ΔM regions for the neutralinos search.

4 Results

4.1 Stable $\tilde{\chi}_1^0$ case

4.1.1 Efficiencies and selected events in the chargino analysis

The total number of background events expected in the different windows is shown in tables 3, 4, 5, 6, together with the number of events selected in the data for the 4 centre–of–mass energies. The method used to compute the asymmetric errors is described in Ref. [8].

The efficiencies of the chargino selection in the four topologies were computed separately for the 104 MSSM points using the $\mathcal{L}_{\mathcal{R}}$ function and the $\mathcal{L}_{\mathcal{R}cut}$ of the corresponding topology and ΔM region. To pass from the efficiencies of the chargino selection in the four topologies to the efficiencies in the four decay channels, all the migration effects were computed for all the generated points of the signal simulation. Then the efficiencies of the selection in the four decay channels were interpolated in the ($M_{\tilde{\chi}_1^\pm}$,$M_{\tilde{\chi}_1^0}$) plane using the same method as in Ref. [8]. When the interpolation was not possible (for $M_{\tilde{\chi}_1^\pm} \sim 80$ GeV/c^2 and $M_{\tilde{\chi}_1^0} \sim 0$ GeV/c^2) an extrapolation was used. These efficiencies as functions of $M_{\tilde{\chi}_1^\pm}$ and $M_{\tilde{\chi}_1^0}$ are shown in Fig. 1 for 200 GeV centre-of-mass energy.

All the selected events in the real data are compatible with the expectation from the background simulation. As no evidence for a signal is found, exclusion limits are set at 95% C.L. using the multichannel Bayesian formula [23] taking into account the branching ratio and the efficiency of each decay channel.

4.1.2 Efficiencies and selected events in the neutralino analysis

The total number of background events expected in the different windows is shown in tables 7, 8, 9, 10, together with the number of events selected in the data for the 4 centre-of mass energies.

The efficiencies of the neutralino selection in the three topologies were computed separately for the 77 mass points points using the $\mathcal{L}_{\mathcal{R}}$ function and the $\mathcal{L}_{\mathcal{R}cut}$ of the corresponding topology and ΔM region. Then the efficiencies of the selection in the three decay channels were interpolated in the ($M_{\tilde{\chi}_1^\pm}$,$M_{\tilde{\chi}_1^0}$) plane using the same method as for the chargino analysis. They can range from 10% to 60% depending on the neutralino masses .

Stable $\tilde{\chi}_1^0$ $E_{cm} = 192$ GeV, $\mathcal{L} = 25.8\ pb^{-1}$

Topology:	$jj\ell$	$\ell\ell$	*jets*	rad	Total
	$3 \leq \Delta M < 5$ GeV/c^2				
Obs. events:	0	9	2	0	11
Expect. events:	$0.09\ ^{+0.33}_{-0.01}$	$8.19\ ^{+0.96}_{-0.65}$	$0.66\ ^{+0.45}_{-0.15}$	$0.65\ ^{+0.37}_{-0.08}$	$9.59\ ^{+1.17}_{-0.68}$
	$5 \leq \Delta M < 10$ GeV/c^2				
Obs. events:	0	4	1	0	5
Expect. events:	$0.10\ ^{+0.33}_{-0.02}$	$3.06\ ^{+0.62}_{-0.31}$	$0.44\ ^{+0.41}_{-0.10}$	$0.65\ ^{+0.37}_{-0.08}$	$4.24\ ^{+0.90}_{-0.34}$
	$10 \leq \Delta M < 25$ GeV/c^2				
Obs. events:	0	5	2	0	7
Expect. events:	$0.19\ ^{+0.34}_{-0.03}$	$4.83\ ^{+0.66}_{-0.36}$	$1.59\ ^{+0.49}_{-0.18}$	$0.65\ ^{+0.37}_{-0.08}$	$7.25\ ^{+0.97}_{-0.41}$
	$25 \leq \Delta M < 35$ GeV/c^2				
Obs. events:	1	4	1	0	6
Expect. events:	$0.27\ ^{+0.33}_{-0.04}$	$4.04\ ^{+0.52}_{-0.25}$	$0.80\ ^{+0.34}_{-0.06}$	$0.65\ ^{+0.37}_{-0.08}$	$5.76\ ^{+0.80}_{-0.27}$
	$35 \leq \Delta M < 50$ GeV/c^2				
Obs. events:	1	4	6	0	11
Expect. events:	$0.21\ ^{+0.33}_{-0.03}$	$4.04\ ^{+0.52}_{-0.25}$	$3.61\ ^{+0.43}_{-0.17}$	$0.56\ ^{+0.36}_{-0.08}$	$8.42\ ^{+0.84}_{-0.32}$
	50 GeV/$c^2 \leq \Delta M$				
Obs. events:	1	4	6	0	11
Expect. events:	$0.21\ ^{+0.33}_{-0.03}$	$4.04\ ^{+0.52}_{-0.25}$	$3.47\ ^{+0.43}_{-0.17}$	$0.56\ ^{+0.36}_{-0.08}$	$8.29\ ^{+0.83}_{-0.31}$
	TOTAL (logical .OR. between different ΔM windows)				
Obs. events:	1	11	9	0	21
Expect. events:	$0.36\ ^{+0.35}_{-0.05}$	$11.80\ ^{+1.02}_{-0.71}$	$4.60\ ^{+0.57}_{-0.28}$	$0.86\ ^{+0.38}_{-0.11}$	$17.63\ ^{+1.28}_{-0.77}$

Table 3: The number of events observed in data and the expected number of background events in the different chargino search channels under the hypothesis of a stable neutralino at 192 GeV of centre–of–mass energy.

Stable $\tilde{\chi}_1^0$ $E_{cm} = 196$ GeV, $\mathcal{L} = 76.8\ pb^{-1}$

Topology:	$jj\ell$	$\ell\ell$	*jets*	rad	Total
	$3 \leq \Delta M < 5$ GeV/c^2				
Obs. events:	0	24	2	0	26
Expect. events:	$0.48\ ^{+0.91}_{-0.07}$	$24.74\ ^{+2.87}_{-1.97}$	$2.01\ ^{+1.32}_{-0.46}$	$1.50\ ^{+0.92}_{-0.13}$	$28.74\ ^{+3.41}_{-2.03}$
	$5 \leq \Delta M < 10$ GeV/c^2				
Obs. events:	0	8	0	0	8
Expect. events:	$0.23\ ^{+0.99}_{-0.04}$	$9.33\ ^{+1.81}_{-0.93}$	$1.34\ ^{+1.19}_{-0.30}$	$1.50\ ^{+0.92}_{-0.13}$	$12.41\ ^{+2.53}_{-0.99}$
	$10 \leq \Delta M < 25$ GeV/c^2				
Obs. events:	0	15	3	0	18
Expect. events:	$0.65\ ^{+0.93}_{-0.08}$	$15.30\ ^{+1.89}_{-1.03}$	$4.82\ ^{+1.39}_{-0.54}$	$1.50\ ^{+0.92}_{-0.13}$	$22.28\ ^{+2.69}_{-1.18}$
	$25 \leq \Delta M < 35$ GeV/c^2				
Obs. events:	0	13	3	0	16
Expect. events:	$1.10\ ^{+0.91}_{-0.10}$	$14.00\ ^{+1.35}_{-0.58}$	$2.40\ ^{+0.91}_{-0.13}$	$1.50\ ^{+0.92}_{-0.13}$	$19.00\ ^{+2.09}_{-0.62}$
	$35 \leq \Delta M < 50$ GeV/c^2				
Obs. events:	0	13	12	0	25
Expect. events:	$0.91\ ^{+0.91}_{-0.07}$	$14.00\ ^{+1.35}_{-0.58}$	$10.55\ ^{+1.06}_{-0.30}$	$0.91\ ^{+0.91}_{-0.08}$	$26.37\ ^{+2.15}_{-0.66}$
	50 GeV/$c^2 \leq \Delta M$				
Obs. events:	0	13	10	0	23
Expect. events:	$0.91\ ^{+0.91}_{-0.07}$	$14.00\ ^{+1.35}_{-0.58}$	$10.22\ ^{+1.06}_{-0.29}$	$0.91\ ^{+0.91}_{-0.08}$	$26.04\ ^{+2.14}_{-0.66}$
	TOTAL (logical .OR. between different ΔM windows)				
Obs. events:	0	36	14	0	50
Expect. events:	$1.27\ ^{+0.942}_{-0.11}$	$37.39\ ^{+2.98}_{-2.08}$	$13.62\ ^{+1.57}_{-0.76}$	$1.74\ ^{+0.92}_{-0.14}$	$54.02\ ^{+3.62}_{-2.22}$

Table 4: The number of events observed in data and the expected number of background events in the different chargino search channels under the hypothesis of a stable neutralino at 196 GeV of centre–of–mass energy.

Stable $\tilde{\chi}_1^0$ $E_{cm} = 200$ GeV, $\mathcal{L} = 83.9\ pb^{-1}$

Topology:	$jj\ell$	$\ell\ell$	*jets*	rad	Total
	$3 \leq \Delta M < 5$ GeV/c^2				
Obs. events:	0	30	4	1	35
Expect. events:	$0.17\ ^{+0.86}_{-0.03}$	$32.15\ ^{+3.06}_{-2.19}$	$2.21\ ^{+1.36}_{-0.51}$	$1.64\ ^{+0.86}_{-0.11}$	$36.17\ ^{+3.56}_{-2.25}$
	$5 \leq \Delta M < 10$ GeV/c^2				
Obs. events:	0	12	2	1	15
Expect. events:	$0.17\ ^{+0.86}_{-0.03}$	$10.70\ ^{+1.83}_{-0.97}$	$1.36\ ^{+1.19}_{-0.34}$	$1.64\ ^{+0.86}_{-0.11}$	$13.87\ ^{+2.50}_{-1.03}$
	$10 \leq \Delta M < 25$ GeV/c^2				
Obs. events:	0	18	1	1	20
Expect. events:	$0.36\ ^{+0.86}_{-0.04}$	$15.99\ ^{+1.89}_{-1.04}$	$3.73\ ^{+1.42}_{-0.59}$	$1.64\ ^{+0.86}_{-0.11}$	$21.73\ ^{+2.66}_{-1.21}$
	$25 \leq \Delta M < 35$ GeV/c^2				
Obs. events:	0	8	2	1	11
Expect. events:	$0.23\ ^{+0.85}_{-0.03}$	$6.23\ ^{+1.05}_{-0.33}$	$2.75\ ^{+0.86}_{-0.12}$	$1.64\ ^{+0.86}_{-0.11}$	$10.85\ ^{+1.82}_{-0.37}$
	$35 \leq \Delta M < 50$ GeV/c^2				
Obs. events:	0	15	8	0	23
Expect. events:	$0.69\ ^{+0.85}_{-0.06}$	$13.32\ ^{+1.22}_{-0.53}$	$8.35\ ^{+1.02}_{-0.25}$	$1.24\ ^{+0.86}_{-0.09}$	$23.60\ ^{+2.00}_{-0.60}$
	50 GeV/$c^2 \leq \Delta M$				
Obs. events:	0	15	11	0	26
Expect. events:	$0.64\ ^{+0.85}_{-0.05}$	$13.32\ ^{+1.22}_{-0.53}$	$11.13\ ^{+1.03}_{-0.28}$	$1.24\ ^{+0.86}_{-0.09}$	$26.34\ ^{+2.01}_{-0.62}$
	TOTAL (logical .OR. between different ΔM windows)				
Obs. events:	0	43	15	1	59
Expect. events:	$0.83\ ^{+0.86}_{-0.07}$	$44.45\ ^{+3.15}_{-2.28}$	$14.60\ ^{+1.64}_{-0.82}$	$2.03\ ^{+0.86}_{-0.12}$	$61.91\ ^{+3.75}_{-2.43}$

Table 5: The number of events observed in data and the expected number of background events in the different chargino search channels under the hypothesis of a stable neutralino at 200 GeV of centre–of–mass energy.

Stable $\tilde{\chi}_1^0$ $E_{cm} = 202$ GeV, $\mathcal{L} = 40.5\ pb^{-1}$

Topology:	$jj\ell$	$\ell\ell$	*jets*	rad	Total
	$3 \leq \Delta M < 5$ GeV/c^2				
Obs. events:	0	22	0	0	22
Expect. events:	$0.06\ ^{+0.44}_{-0.01}$	$15.72\ ^{+1.49}_{-1.06}$	$1.07\ ^{+0.67}_{-0.24}$	$0.64\ ^{+0.46}_{-0.08}$	$17.48\ ^{+1.76}_{-1.09}$
	$5 \leq \Delta M < 10$ GeV/c^2				
Obs. events:	0	7	0	0	7
Expect. events:	$0.06\ ^{+0.44}_{-0.01}$	$5.31\ ^{+0.91}_{-0.47}$	$0.66\ ^{+0.59}_{-0.16}$	$0.64\ ^{+0.46}_{-0.08}$	$6.66\ ^{+1.26}_{-0.51}$
	$10 \leq \Delta M < 25$ GeV/c^2				
Obs. events:	0	9	3	0	12
Expect. events:	$0.15\ ^{+0.45}_{-0.08}$	$7.67\ ^{+0.92}_{-0.54}$	$1.79\ ^{+0.70}_{-0.28}$	$0.64\ ^{+0.46}_{-0.08}$	$10.25\ ^{+1.35}_{-0.61}$
	$25 \leq \Delta M < 35$ GeV/c^2				
Obs. events:	0	4	2	0	6
Expect. events:	$0.30\ ^{+0.45}_{-0.05}$	$3.00\ ^{+0.58}_{-0.24}$	$1.45\ ^{+0.45}_{-0.08}$	$0.64\ ^{+0.46}_{-0.08}$	$5.38\ ^{+0.98}_{-0.27}$
	$35 \leq \Delta M < 50$ GeV/c^2				
Obs. events:	0	7	8	1	16
Expect. events:	$0.32\ ^{+0.44}_{-0.06}$	$6.22\ ^{+0.70}_{-0.37}$	$4.11\ ^{+0.55}_{-0.18}$	$0.54\ ^{+0.46}_{-0.07}$	$11.20\ ^{+1.09}_{-0.43}$
	50 GeV/$c^2 \leq \Delta M$				
Obs. events:	0	7	9	1	17
Expect. events:	$0.32\ ^{+0.44}_{-0.06}$	$6.22\ ^{+0.70}_{-0.37}$	$5.59\ ^{+0.56}_{-0.22}$	$0.54\ ^{+0.46}_{-0.07}$	$12.67\ ^{+1.10}_{-0.45}$
	TOTAL (logical .OR. between different ΔM windows)				
Obs. events:	0	27	10	1	38
Expect. events:	$0.37\ ^{+0.45}_{-0.06}$	$21.27\ ^{+1.57}_{-1.13}$	$7.20\ ^{+0.83}_{-0.43}$	$0.80\ ^{+0.47}_{-0.09}$	$29.65\ ^{+1.89}_{-1.22}$

Table 6: The number of events observed in data and the expected number of background events in the different chargino search channels under the hypothesis of a stable neutralino at 202 GeV of centre–of–mass energy.

E_{cm} = 192 GeV, $\mathcal{L}$ = 25.8 pb^{-1}

Topology:	ee	mm	qq	Total
	$0 \leq E_{vis} < 20$ GeV			
Obs. events:	1	9	8	18
Expect. events:	0.1	8.9	7.8	16.8
	$20 \leq E_{vis} < 40$ GeV			
Obs. events:	4	2	2	8
Expect. events:	0.5	1.3	1.1	2.9
	$40 \leq E_{vis} < 60$ GeV			
Obs. events:	1	4	3	8
Expect. events:	2.8	1.8	1.6	6.2
	$60 \leq E_{vis} < 90$ GeV			
Obs. events:	3	2	1	6
Expect. events:	4.6	2.7	2.4	9.7
	$60 \leq E_{vis} < 90$ GeV			
Obs. events:	3	7	5	15
Expect. events:	4.0	3.1	1.4	8.5
	TOTAL			
Obs. events:	12	24	19	55
Expect. events:	$12\ ^{+3.59}_{-2.00}$	$17.8\ ^{+2.81}_{-2.20}$	$14.3\ ^{+2.53}_{-2.11}$	$44.1\ ^{+4.23}_{-3.61}$

Table 7: The number of events observed in data and the expected number of background events in the different neutralino search channels at 192 GeV of centre–of–mass energy.

E_{cm} = 196 GeV, $\mathcal{L}$ = 76.8 pb^{-1}

Topology:	ee	mm	qq	Total
	$0 \leq E_{vis} < 20$ GeV			
Obs. events:	0	5	11	16
Expect. events:	0.2	3.2	10.3	13.7
	$20 \leq E_{vis} < 40$ GeV			
Obs. events:	8	1	2	11
Expect. events:	5.2	3.8	0.6	9.6
	$40 \leq E_{vis} < 60$ GeV			
Obs. events:	3	4	4	11
Expect. events:	2.1	3.2	8.1	13.4
	$60 \leq E_{vis} < 90$ GeV			
Obs. events:	4	4	30	38
Expect. events:	6.6	7.0	23.3	36.9
	$60 \leq E_{vis} < 90$ GeV			
Obs. events:	7	4	12	23
Expect. events:	5.3	7.3	11.7	24.3
	TOTAL			
Obs. events:	22	18	59	99
Expect. events:	$19.4\ ^{+5.58}_{-2.02}$	$24.5\ ^{+5.27}_{-2.57}$	$54.0\ ^{+5.34}_{-4.00}$	$97.9\ ^{+7.49}_{-5.78}$

Table 8: The number of events observed in data and the expected number of background events in the different neutralino search channels at 196 GeV of centre–of–mass energy.

E_{cm} = 200 GeV, $\mathcal{L}$ = 83.9 pb^{-1}

Topology:	ee	mm	qq	Total
	$0 \leq E_{vis} < 20$ GeV			
Obs. events:	13	8	1	22
Expect. events:	20.2	5.2	3.7	29.1
	$20 \leq E_{vis} < 40$ GeV			
Obs. events:	4	1	3	8
Expect. events:	1.5	3.2	0.7	5.4
	$40 \leq E_{vis} < 60$ GeV			
Obs. events:	1	4	7	12
Expect. events:	6.0	2.0	6.1	14.1
	$60 \leq E_{vis} < 90$ GeV			
Obs. events:	7	3	18	28
Expect. events:	5.0	5.0	16.0	26.0
	$60 \leq E_{vis} < 90$ GeV			
Obs. events:	11	6	15	32
Expect. events:	6.5	6.3	14.4	27.2
	TOTAL			
Obs. events:	36	22	44	102
Expect. events:	$39.2\ ^{+9.94}_{-6.8}$	$21.7\ ^{+5.00}_{-2.79}$	$40.9\ ^{+4.45}_{-2.85}$	$101.8\ ^{+11.41}_{-8.84}$

Table 9: The number of events observed in data and the expected number of background events in the different neutralino search channels at 200 GeV of centre–of–mass energy.

E_{cm} = 202 GeV, $\mathcal{L}$ = 40.5 pb^{-1}

Topology:	ee	mm	qq	Total
	$0 \leq E_{vis} < 20$ GeV			
Obs. events:	2	6	2	10
Expect. events:	8.3	6.1	6.4	20.8
	$20 \leq E_{vis} < 40$ GeV			
Obs. events:	1	2	1	4
Expect. events:	0.6	4.6	0.9	6.1
	$40 \leq E_{vis} < 60$ GeV			
Obs. events:	2	3	3	8
Expect. events:	3.6	2.0	2.3	7.9
	$60 \leq E_{vis} < 90$ GeV			
Obs. events:	9	6	10	25
Expect. events:	3.0	4.0	11.4	18.4
	$60 \leq E_{vis} < 90$ GeV			
Obs. events:	9	7	10	26
Expect. events:	4.7	4.6	11.6	20.9
	TOTAL			
Obs. events:	23	24	26	73
Expect. events:	$20.2\ ^{+4.53}_{-3.00}$	$21.3\ ^{+6.16}_{-3.45}$	$32.6\ +3.91_{-2.59}$	$74.1\ ^{+7.84}_{-6.05}$

Table 10: The number of events observed in data and the expected number of background events in the different neutralino search channels at 202 GeV of centre–of–mass energy.

All the selected events in the real data are compatible with the expectation from the background simulation.

4.1.3 Limits

Limits on chargino production

The simulated points were used to parametrize the efficiencies of the chargino selection criteria described in section 3.2 in terms of ΔM and the mass of the chargino (see section 4.1.1). Then a large number of SUSY points were investigated and the values of ΔM, the chargino and neutralino masses and the various decay branching ratios were determined for each point. By applying the appropriate efficiency (from the interpolation) and branching ratios and cross-sections for each channel decay (computed by SUSYGEN), the number of expected signal events can be calculated. Taking into account the expected background and the number of observed events, the corresponding point in the MSSM parameter space (μ, M_2, $\tan\beta$) can be excluded if the number of expected signal events is greater than the upper limit at 95% C.L. on the number of observed events of the corresponding ΔM region.

Fig. 2 shows the chargino production cross-sections as obtained in the MSSM at $\sqrt{s} = 202$ GeV for different chargino masses for the non-degenerate ($\Delta M > 10$ GeV/c^2) and degenerate cases ($\Delta M = 3$ GeV/c^2) . The parameters M_2 and μ were varied randomly in the ranges 0 GeV/c^2 $< M_2 <$ 3000 GeV/c^2 and –200 GeV/c^2 $< \mu <$ 200 GeV/c^2 for three fixed different values of $\tan\beta$, namely 1, 1.5 and 35. The random generation of the parameters led to an accuracy on the mass limit computation of the order of 10 MeV/c^2. Two different cases were considered for the sneutrino mass: $M_{\tilde{\nu}} > 300$ GeV/c^2 (in the non-degenerate case) and $M_{\tilde{\nu}} > M_{\tilde{\chi}_1^\pm}$ (in the degenerate case).

To derive the chargino mass limits, constraints on the process $Z \to \tilde{\chi}_1^0\tilde{\chi}_2^0 \to \tilde{\chi}_1^0\tilde{\chi}_1^0\gamma$ were also included. These were derived from the DELPHI results on single-photon production at LEP 1 [24].

The chargino mass limits are summarized in Table 11. The table also gives, for each case, the minimal MSSM cross-section for which $M_{\tilde{\chi}_1^\pm}$ is below the corresponding mass limit. These cross-section values are also displayed in Fig. 2. The chargino mass limits versus ΔM assuming a heavy sneutrino, is shown in Fig. 3. The behaviour of the curve in Fig. 3 depends very weakly on the relation between M_1 and M_2.

In the non-degenerate case ($\Delta M > 10$ GeV/c^2) with a large sneutrino mass (> 300 GeV/c^2), the lower limit for the chargino ranges between 99.6 GeV/c^2 (for a mostly higgsino-like chargino) and 100.5 GeV/c^2 (for a mostly wino-like chargino). The minimal excluded MSSM cross-section at $\sqrt{s} = 202$ GeV is 0.48 pb, deriving from a chargino mass limit of 99.5 GeV/c^2. For $\Delta M > 20$ GeV/c^2, the lower limit for the chargino mass ranges between 99.6 GeV/c^2 and 100.5 GeV/c^2. In this case the minimum excluded MSSM cross-section at $\sqrt{s} = 202$ GeV is 0.47 pb.

In the degenerate case ($\Delta M = 3$ GeV/c^2), the cross-section does not depend significantly on the sneutrino mass, since the chargino is higgsino-like under the assumption of gaugino mass unification. The lower limit for the chargino mass, shown in Fig. 2, is 95.0 GeV/c^2. The minimal excluded cross–section is in this case 1.18 pb at $\sqrt{s} = 202$ GeV.

The systematic error on the given mass limits is less than 0.5% for $\Delta M = 3$ GeV/c^2 and less than 0.1% for $\Delta M > 20$ GeV/c^2, the method used to compute these systematic errors is similar as at $\sqrt{s} = 189$ GeV [8].

Case	$m_{\tilde{\nu}}$ (GeV/c^2)	$M^{min}_{\chi^\pm}$ (GeV/c^2)	σ^{max} (pb)	$\mathrm{N}_{95\%}$
Stable $\tilde{\chi}^0_1$ E_{cm} = 196-202 GeV				
$\Delta M > 20$ GeV/c^2	> 300	99.6	0.47	6.7
$\Delta M > 10$ GeV/c^2	> 300	99.5	0.48	6.9
$\Delta M = 3$ GeV/c^2	$>M_{\tilde{\chi}^\pm_1}$	95.0	1.18	14.8
Unstable $\tilde{\chi}^0_1$ E_{cm} = 202 GeV				
$\Delta M > 10$ GeV/c^2	> 300	99.7	0.44	5.14
$\Delta M = 1$ GeV/c^2	$>M_{\tilde{\chi}^\pm_1}$	100.4	0.24	3.09

Table 11: 95% confidence level lower limits for the chargino mass, the corresponding pair production cross-sections until 202 GeV and the 95% confidence level upper limit on number of observed events, for the non-degenerate and a highly degenerate cases. The scenarios of a stable $\tilde{\chi}^0_1$ and $\tilde{\chi}^0_1 \rightarrow \tilde{\mathrm{G}}\gamma$ are considered.

Limits on MSSM parameters and neutralino mass

The exclusion regions in the (μ, M_2) plane for $\tan\beta$ = 1, 1.5 and 35 are shown in Fig. 4.a, 4.b, and 4.c, assuming a heavy sneutrino. These limits, based on data taken at $\sqrt{s} \leq 202$ GeV, improve previous limits at lower energies.

DELPHI limits on the process $\mathrm{Z} \rightarrow \tilde{\chi}^0_1\tilde{\chi}^0_2 \rightarrow \tilde{\chi}^0_1\tilde{\chi}^0_1\gamma$ at LEP 1 [24] marginally extends part of the region covered by the chargino search at low $\tan\beta$ for small M_2 and negative μ (Fig. 4.d). The exclusion region obtained depends strongly on the the assumed GUT relation between M_1 and M_2.

A lower limit of 35.2 GeV/c^2 on the lighest neutralino mass is obtained, valid for $\tan\beta \geq 1$ and a heavy sneutrino. This limit is reached for $\tan\beta = 1$, $\mu = -59.6$ GeV/c^2, $\mathrm{M}_2 = 59.4$ GeV/c^2.

Limits on neutralino production

As no evidence for a signal is found, model independent upper limits are set at 95% C.L. on the production cross–section times branching fraction in the neutralino mass plane ($M_{\tilde{\chi}^0_2}$,$M_{\tilde{\chi}^0_1}$) for each topology at each centre–of–mass energy. For each channel the multichannel Bayesian formula has been used to compute the limits taking into account

the efficiency and number of events in each ΔM region. The results obained are shown in fig. 5-8

4.2 Unstable $\tilde{\chi}_1^0$ case

4.2.1 Efficiencies and selected events

The efficiency of the chargino selection for an unstable $\tilde{\chi}_1^0$ decaying into a photon and a gravitino was calculated from a total of 78000 events generated using the same combinations of $M_{\tilde{\chi}_1^\pm}$ and $M_{\tilde{\chi}_1^0}$ as in the stable $\tilde{\chi}_1^0$ scenario. As mentioned in [8], the same selection applies to all topologies. Only three ΔM windows were used in the Gravitino LSP scenario. Note that, due to the presence of the photons from the neutralino decay, the region of high degeneracy (down to $\Delta M = 1$ GeV/c^2) is fully covered.

The total number of background events expected in the three different ΔM ranges is shown in table 12, together with the number of events selected in the data for the 4 centre-of-mass energies. Since no evidence for a signal was found, exclusion limits were set.

4.2.2 Limits

The chargino cross-section limits corresponding to the case where the neutralino is unstable and decays via $\tilde{\chi}_1^0 \rightarrow \tilde{\mathrm{G}}\gamma$ were computed at $\sqrt{s} = 202$ GeV as explained in section 4.1.3 and are shown in Fig. 2 and in table 11. In the non-degenerate case the chargino mass limit at 95% C.L. is 99.7 GeV/c^2 for a heavy sneutrino, while in the ultra-degenerate case ($\Delta M = 1$ GeV/c^2) the limit is 100.4 GeV/c^2. The minimal MSSM cross-sections excluded by the above mass limits are 0.44 pb in the non-degenerate case and 0.24 pb in the ultra-degenerate case.

5 Summary

Searches for charginos and neutralinos at $\sqrt{s} \leq 202$ GeV allow the exclusion of a large domain of SUSY parameters, cross-sections, and masses, at 95% confidence level.

Assuming a difference in mass between chargino and neutralino, ΔM, of 10 GeV/c^2 or more, and a sneutrino heavier than 300 GeV/c^2, the existence of a chargino lighter than 99.5 GeV/c^2 can be excluded. If a gaugino-dominated chargino is assumed in addition, the kinematic limit is reached. If ΔM is 3 GeV/c^2, the lower limit on the chargino mass becomes 95.0 GeV/c^2, assuming a sneutrino heavier than the chargino.

A lower limit of 35.2 GeV/c^2 on the lightest neutralino mass is obtained assuming a heavy sneutrino and $M_1/M_2 \approx 0.5$, using the obtained chargino exclusion regions and including DELPHI results [24] on the process $\mathrm{Z} \rightarrow \tilde{\chi}_1^0\tilde{\chi}_2^0 \rightarrow \tilde{\chi}_1^0\tilde{\chi}_1^0\gamma$.

A specific $\tilde{\chi}_1^+\tilde{\chi}_1^-$ production search was performed assuming the decay of the lightest neutralino into a photon and a gravitino, giving somewhat more stringent limits on cross-sections and masses than in the case of a stable $\tilde{\chi}_1^0$: $M_{\tilde{\chi}_1^\pm} > 99.7$ GeV/c^2 for large ΔM and $M_{\tilde{\chi}_1^\pm} > 100.4$ GeV/c^2 for $\Delta M = 1$ GeV/c^2.

Searches for neutralino allow to put model independent upper limits on the production cross–section times branching fraction of neutralino events.

Unstable $\tilde{\chi}_1^0$	$E_{cm} = 192$ GeV, $\mathcal{L} = 25.8\ pb^{-1}$		
	$\Delta M > 10$ GeV/c^2	$5 \leq \Delta M \leq 10$ GeV/c^2	$\Delta M < 5$ GeV/c^2
Obs. events:	3	0	0
Expect. events:	$2.42\ ^{+0.46}_{-0.22}$	$0.33\ ^{+0.35}_{-0.05}$	$0.22\ ^{+0.35}_{-0.03}$
Unstable $\tilde{\chi}_1^0$	$E_{cm} = 196$ GeV, $\mathcal{L} = 76.8\ pb^{-1}$		
	$\Delta M > 10$ GeV/c^2	$5 \leq \Delta M \leq 10$ GeV/c^2	$\Delta M < 5$ GeV/c^2
Obs. events:	5	1	1
Expect. events:	$7.28\ ^{+0.97}_{-0.30}$	$1.21\ ^{+0.92}_{-0.13}$	$0.90\ ^{+0.94}_{-0.11}$
Unstable $\tilde{\chi}_1^0$	$E_{cm} = 200$ GeV, $\mathcal{L} = 83.9\ pb^{-1}$		
	$\Delta M > 10$ GeV/c^2	$5 \leq \Delta M \leq 10$ GeV/c^2	$\Delta M < 5$ GeV/c^2
Obs. events:	2	2	2
Expect. events:	$6.84\ ^{+0.89}_{-0.23}$	$1.02\ ^{+0.86}_{-0.09}$	$0.60\ ^{+0.85}_{-0.06}$
Unstable $\tilde{\chi}_1^0$	$E_{cm} = 202$ GeV, $\mathcal{L} = 40.5\ pb^{-1}$		
	$\Delta M > 10$ GeV/c^2	$5 \leq \Delta M \leq 10$ GeV/c^2	$\Delta M < 5$ GeV/c^2
Obs. events:	3	0	0
Expect. events:	$3.07\ ^{+0.52}_{-0.22}$	$0.38\ ^{+0.45}_{-0.06}$	$0.25\ ^{+0.44}_{-0.04}$

Table 12: The number of events observed and the expected number of background events in the different ΔM cases under the hypothesis of an unstable $\tilde{\chi}_1^0$ for the 4 centre-of-mass energies (section 3.2).

References

[1] P. Fayet and S. Ferrara, Phys. Rep. **32** (1977) 249;
H.P. Nilles, Phys. Rep. **110** (1984) 1;
H.E. Haber and G.L. Kane, Phys. Rep. **117** (1985) 75.

[2] DELPHI Coll., P. Abreu *et al.*, Eur. Phys. J. **C1** (1998) 1-20.

[3] DELPHI Coll., P. Aarnio *et al.*, Nucl. Instr. and Meth. **303** (1991) 233;
DELPHI Coll., P. Abreu *et al.*, Nucl. Instr. and Meth. **378** (1996) 57.

[4] T.W. Anderson, An Introduction to multivariate analysis, New York Wiley, 1958.

[5] D. Dicus *et al.*, Phys. Rev. **D41** (1990) 2347;
D. Dicus *et al.*, Phys. Rev. **D43** (1991) 2951;
D. Dicus *et al.*, Phys. Lett. **B258** (1991) 231.

[6] S. Dimopoulos *et al.*, Phys. Rev. Lett. **76** (1996) 3494;
S. Ambrosanio *et al.*, Phys. Rev. Lett. **76** (1996) 3498;
J.L. Lopez and D.V. Nanopoulos, Mod. Phys. Lett. **A10** (1996) 2473;
J.L. Lopez and D.V. Nanopoulos, Phys. Rev. **D55** (1997) 4450.

[7] S. Ambrosanio *et al.*, Phys. Rev. **D54** (1996) 5395.

[8] T. Alderweireld, I. Gil, P. Rebecchi, *Review of the chargino search in DELPHI. Latest results at $E_{\rm cm}$ = 189 GeV*, DELPHI note 99-177 PHYS 843 (1999).
[9] T. Sjöstrand, Comp. Phys. Comm. **39** (1986) 347;
T. Sjöstrand, `PYTHIA 5.6` *and* `JETSET 7.3`, CERN-TH/6488-92.
[10] DELPHI Coll., P. Abreu *et al.*, Z. Phys. **C73** (1996) 11.
[11] S. Katsanevas and P. Morawitz, Comp. Phys. Comm. **112** (1998) 227.
[12] S. Ambrosanio and B. Mele, Phys. Rev. **D52** (1995) 3900;
S. Ambrosanio and B. Mele, Phys. Rev. **D53** (1996) 2451.
[13] J.E. Campagne and R. Zitoun, Z. Phys. **C43** (1989) 469.
[14] S. Jadach, B.F.L. Ward and Z. Was, Comp. Phys. Comm. **79** (1994) 503.
[15] F.A. Berends, R. Kleiss, W. Hollik, Nucl. Phys. **B304** (1988) 712.
[16] F.A. Berends, R. Pittau, R. Kleiss, Comp. Phys. Comm. **85** (1995) 437.
[17] J.Fujimoto *et al.*, Comp. Phys. Comm. **100** (1997) 128
[18] S. Nova, A. Olshevski, and T. Todorov, *A Monte Carlo event generator for two photon physics*, DELPHI note 90-35 (1990).
[19] F.A. Berends, P.H. Daverveldt, R. Kleiss, Comp. Phys. Comm. **40** (1986) 271, Comp. Phys. Comm. **40** (1986) 285, Comp. Phys. Comm. **40** (1986) 309.
[20] P. Abreu *et al.*, DELPHI note, DELPHI 96-124 PHYS
[21] S. Catani *et al.*, Phys. Lett. **B269** (1991) 432;
N.Brown and W.J. Stirling Z. Phys. **C53** (1992) 629.
[22] A.V. Oppenheim and R.W. Schafer, Discrete-time signal processing, Prentice-Hall, 1989
[23] V.F. Obraztsov, Nucl. Instr. and Meth. **316** (1992) 388;
V.F. Obraztsov, Nucl. Instr. and Meth. **399** (1997) 500.
[24] DELPHI Coll., P. Abreu *et al.*, Z. Phys. **C74** (1997) 577

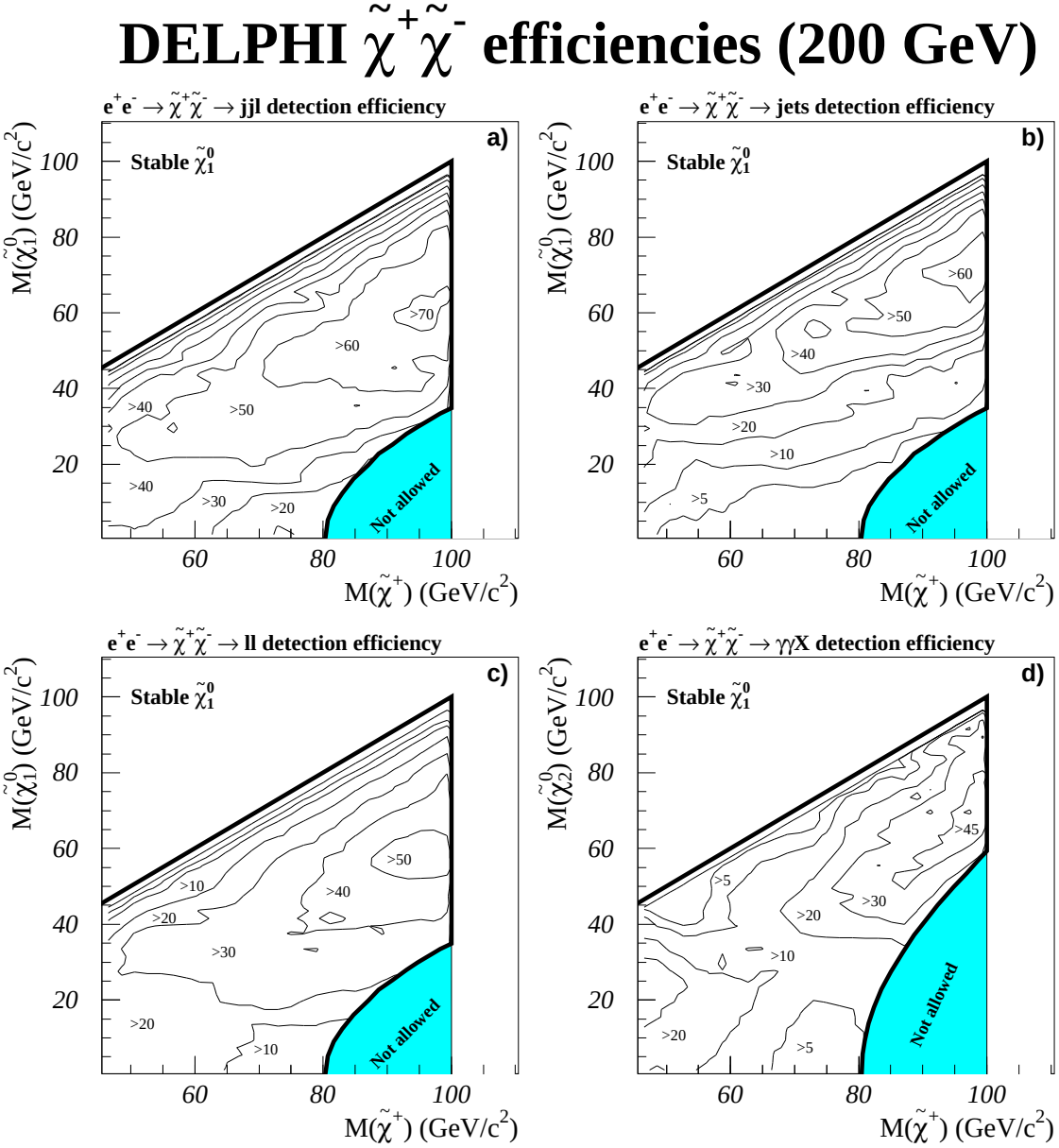

Figure 1: Chargino pair production detection efficiencies (%) for the four decay channels a) $jj\ell$, b) *jets*, c) $\ell\ell$ and d) *rad*, at 200 GeV in the $(M_{\tilde{\chi}^\pm}, M_{\tilde{\chi}^0})$ plane. A stable $\tilde{\chi}_1^0$ is assumed. The shaded areas are disallowed in the MSSM scheme.

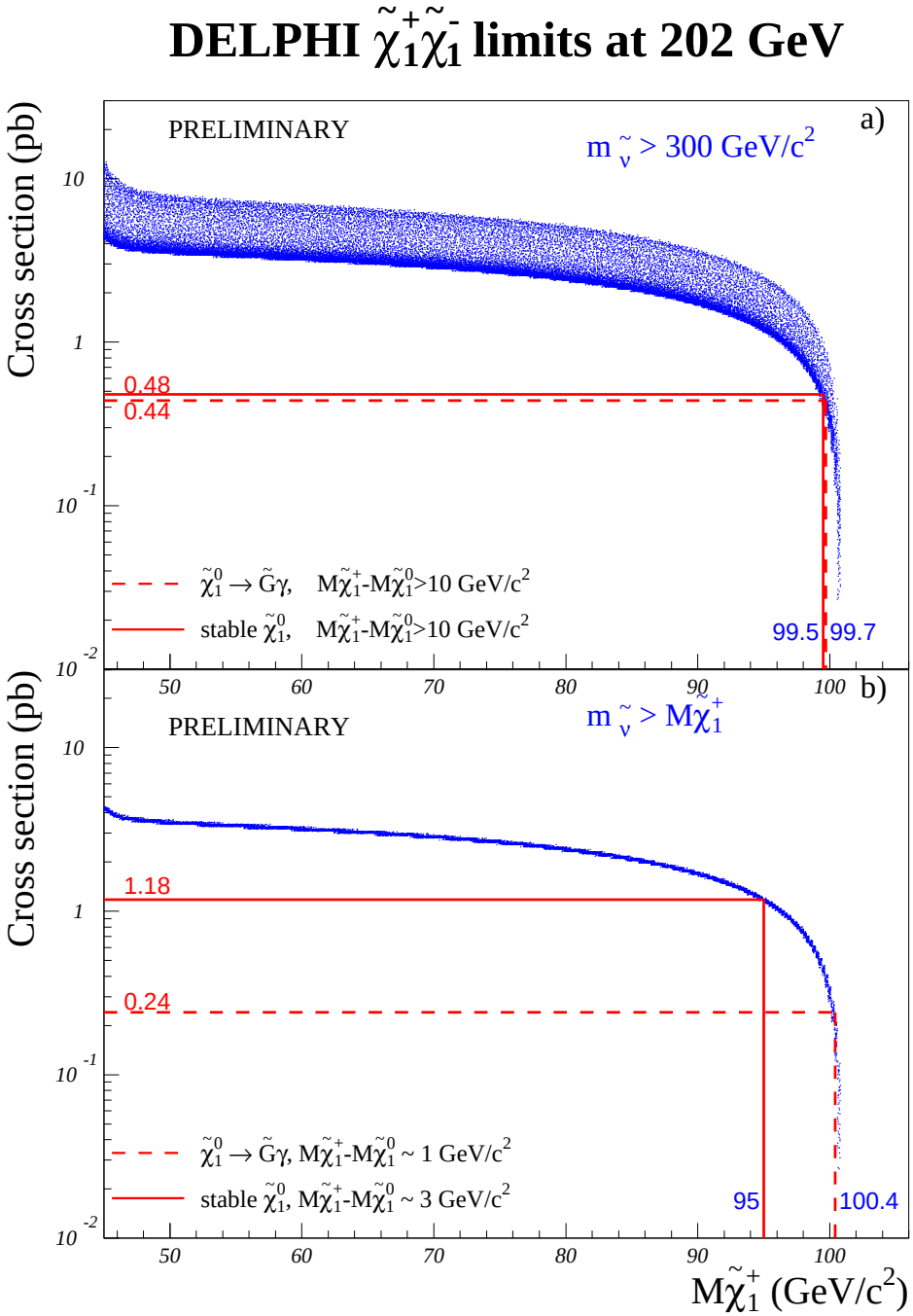

Figure 2: Expected cross-sections in pb at 202 GeV (dots) versus the chargino mass in a) in the non-degenerate case ($\Delta M > 10$ GeV/c^2) and b) the degenerate case ($\Delta M \sim 3$ GeV/c^2). The spread in the dots originates from the random scan over the parameters μ and M_2. A heavy sneutrino ($m_{\tilde{\nu}} > 300$ GeV/c^2) has been assumed in a) and $m_{\tilde{\nu}} > M_{\tilde{\chi}_1^\pm}$ in b). The minimal cross-sections below the mass limits are indicated by the horizontal lines.

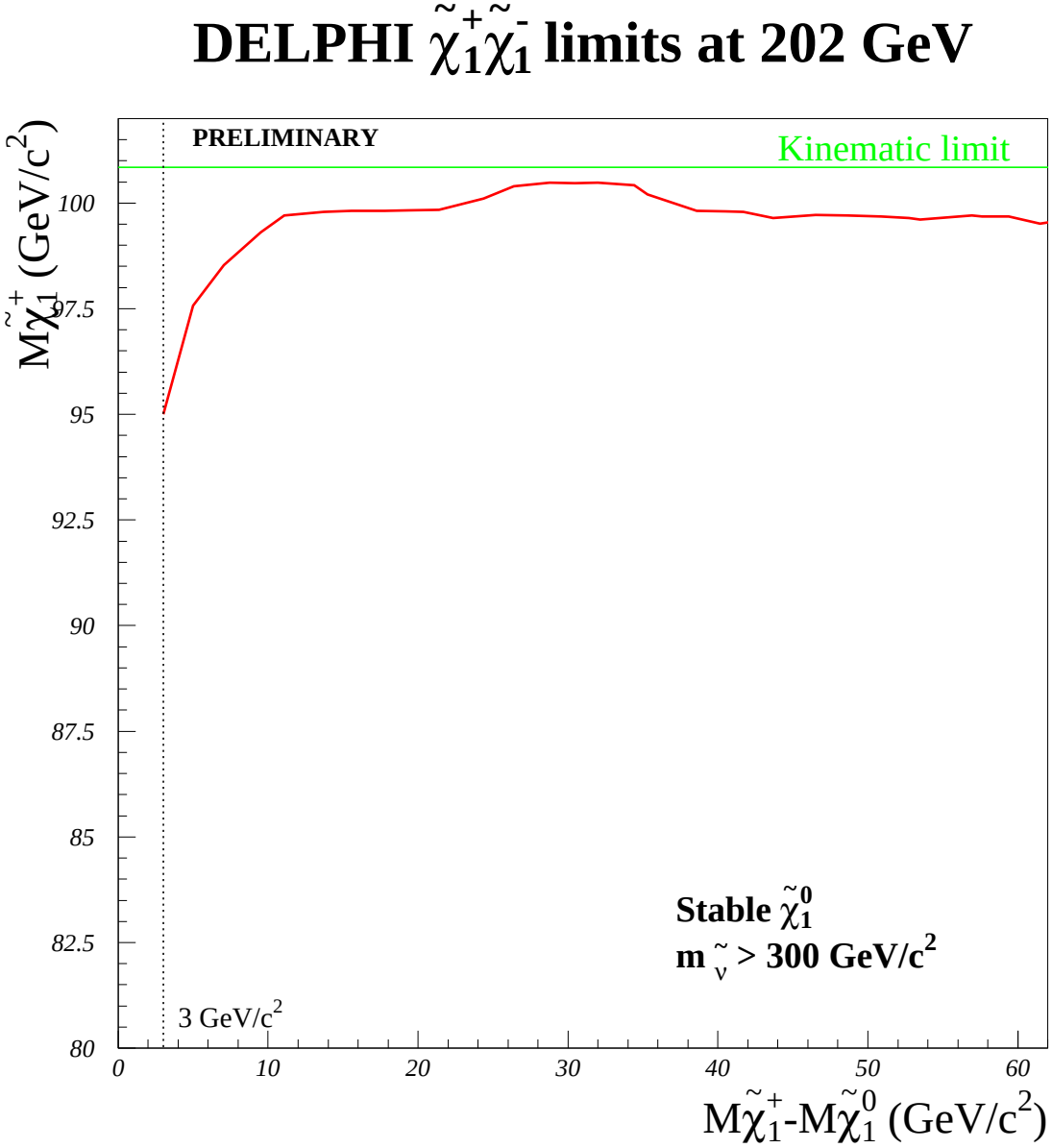

Figure 3: The chargino mass limit as function of the ΔM value under the assumption of a heavy sneutrino. The limit applies to the case of a stable $\tilde{\chi}_1^0$. The straight horizontal line shows the kinematic limit.

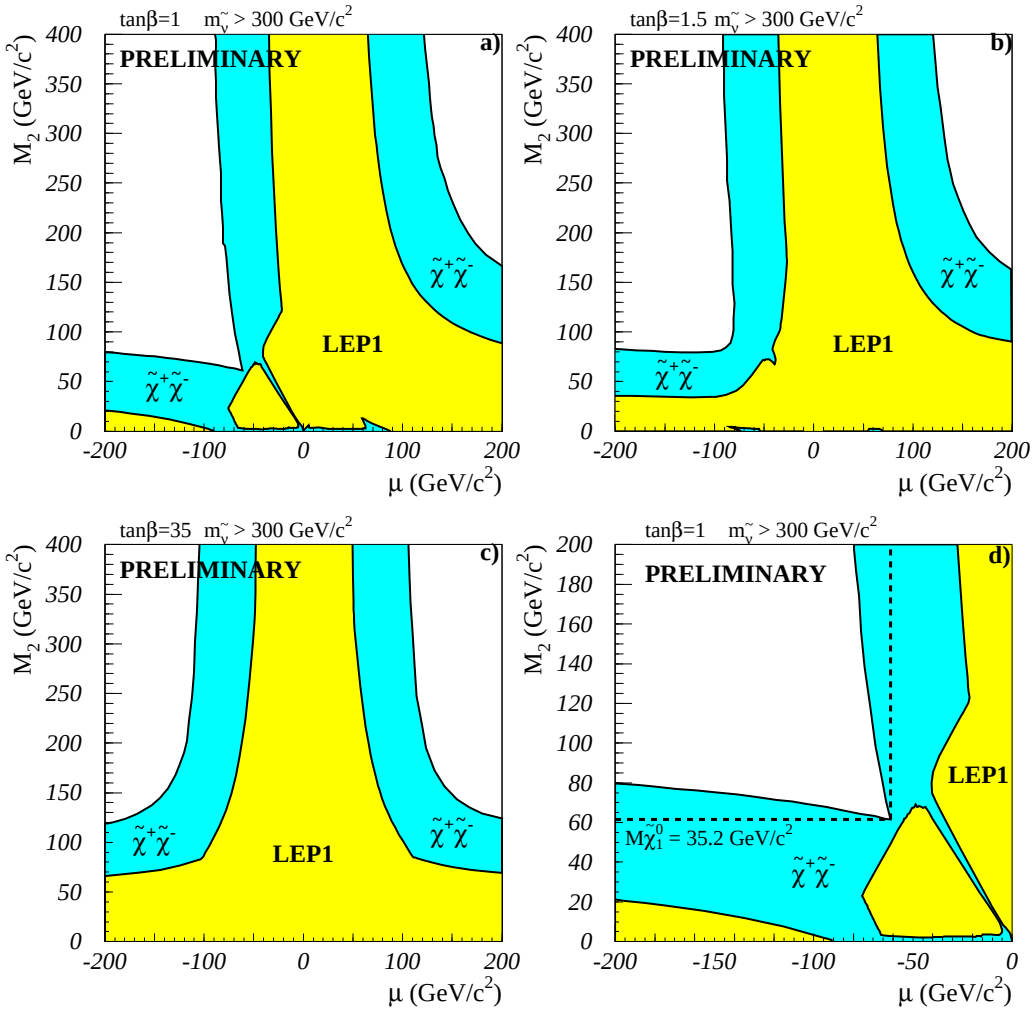

Figure 4: a), b), and c), regions excluded at 95 % confidence level in the (μ, M_2) plane under the assumption of a heavy sneutrino for $\tan\beta = 1$, 1.5 and 35. The dark shading shows the region excluded by the chargino search and the light shaded region is the one excluded by LEP1. The constant mass curve for the LSP mass limit is shown in d) by the dashed line, for $\tan\beta = 1$.

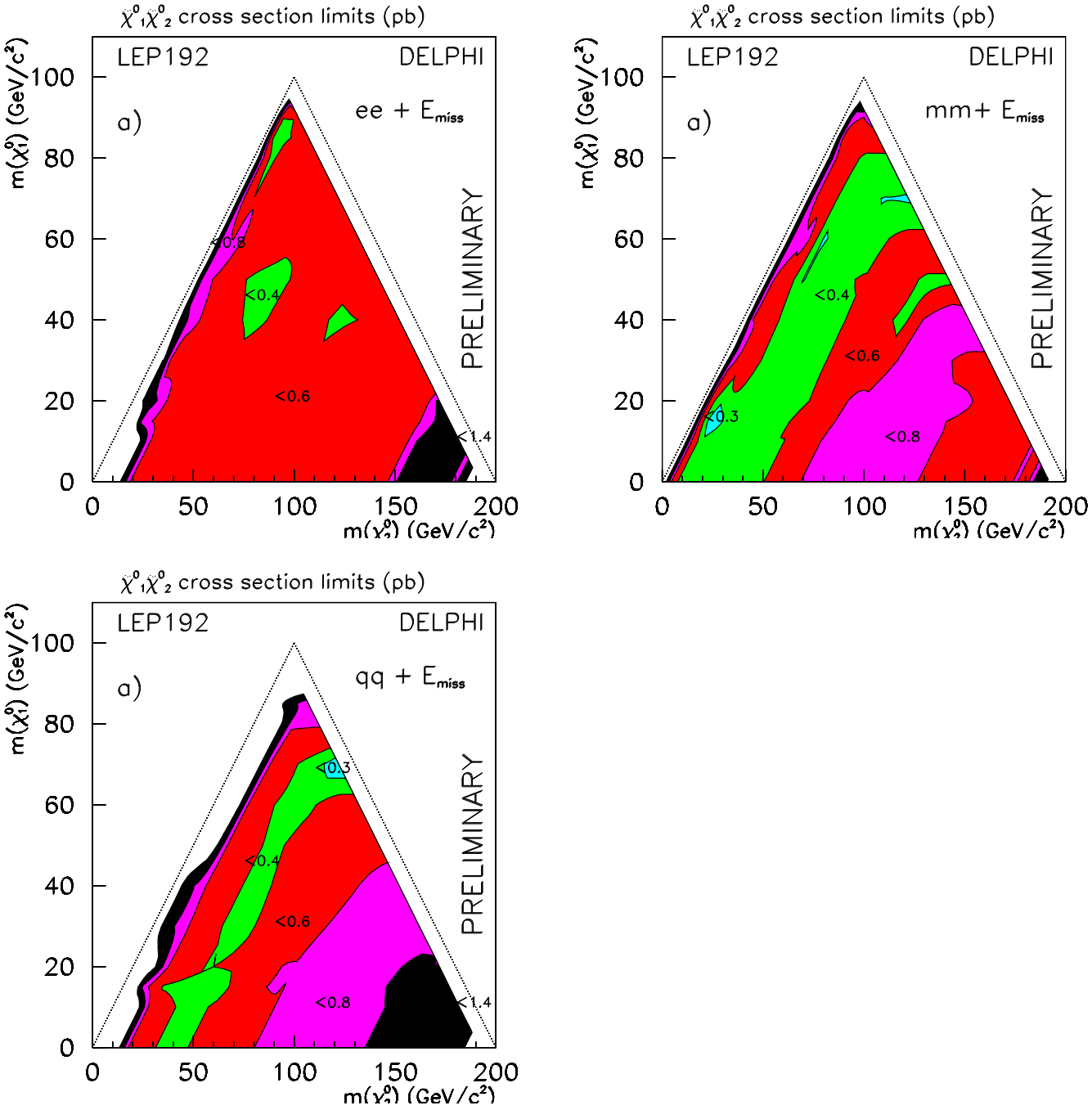

Figure 5: Upper limit on the cross–section times branching ractio for different neutralino search channel at 192 GeV

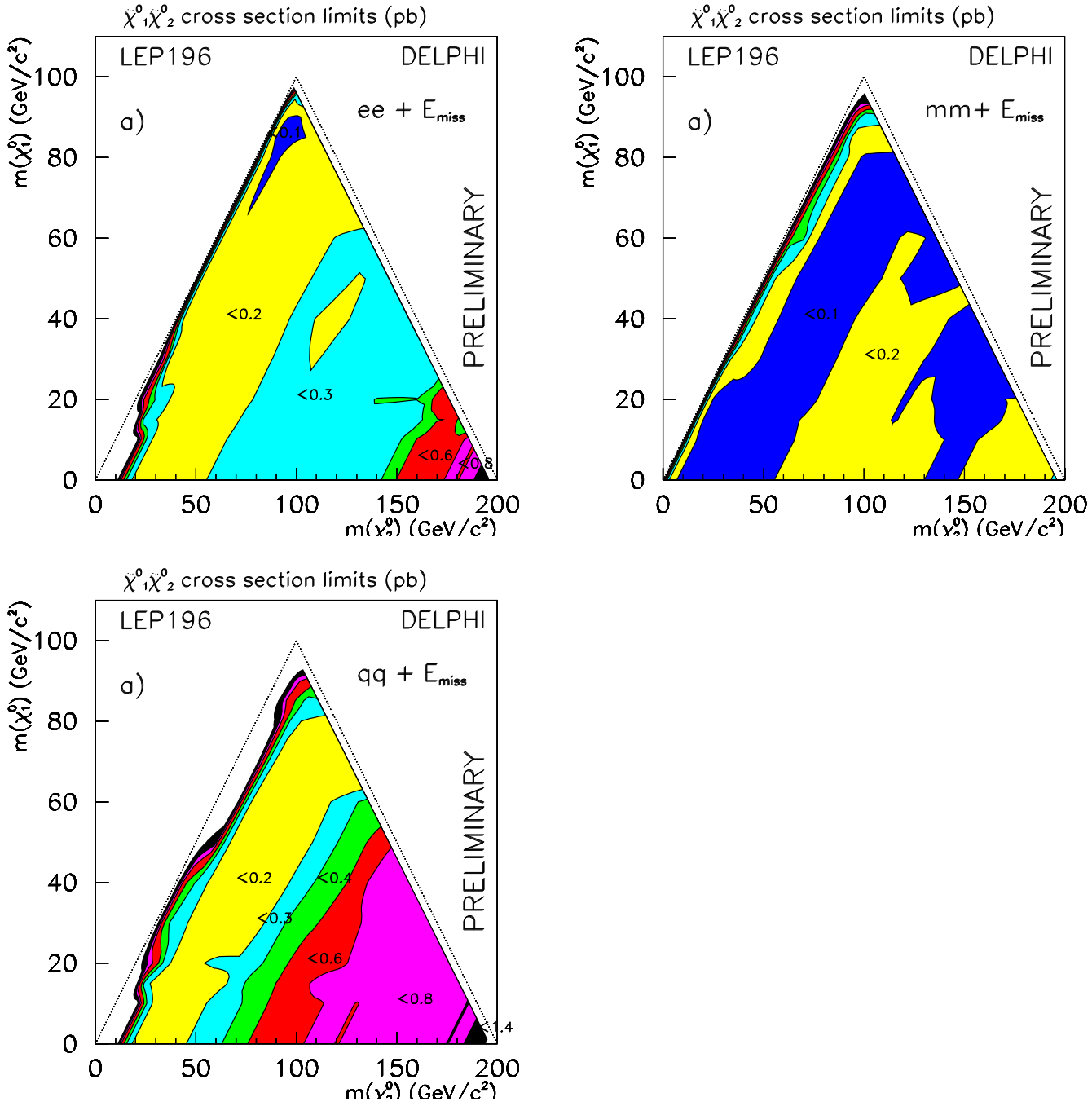

Figure 6: Upper limit on the cross–section times branching ractio for different neutralino search channel at 196 GeV

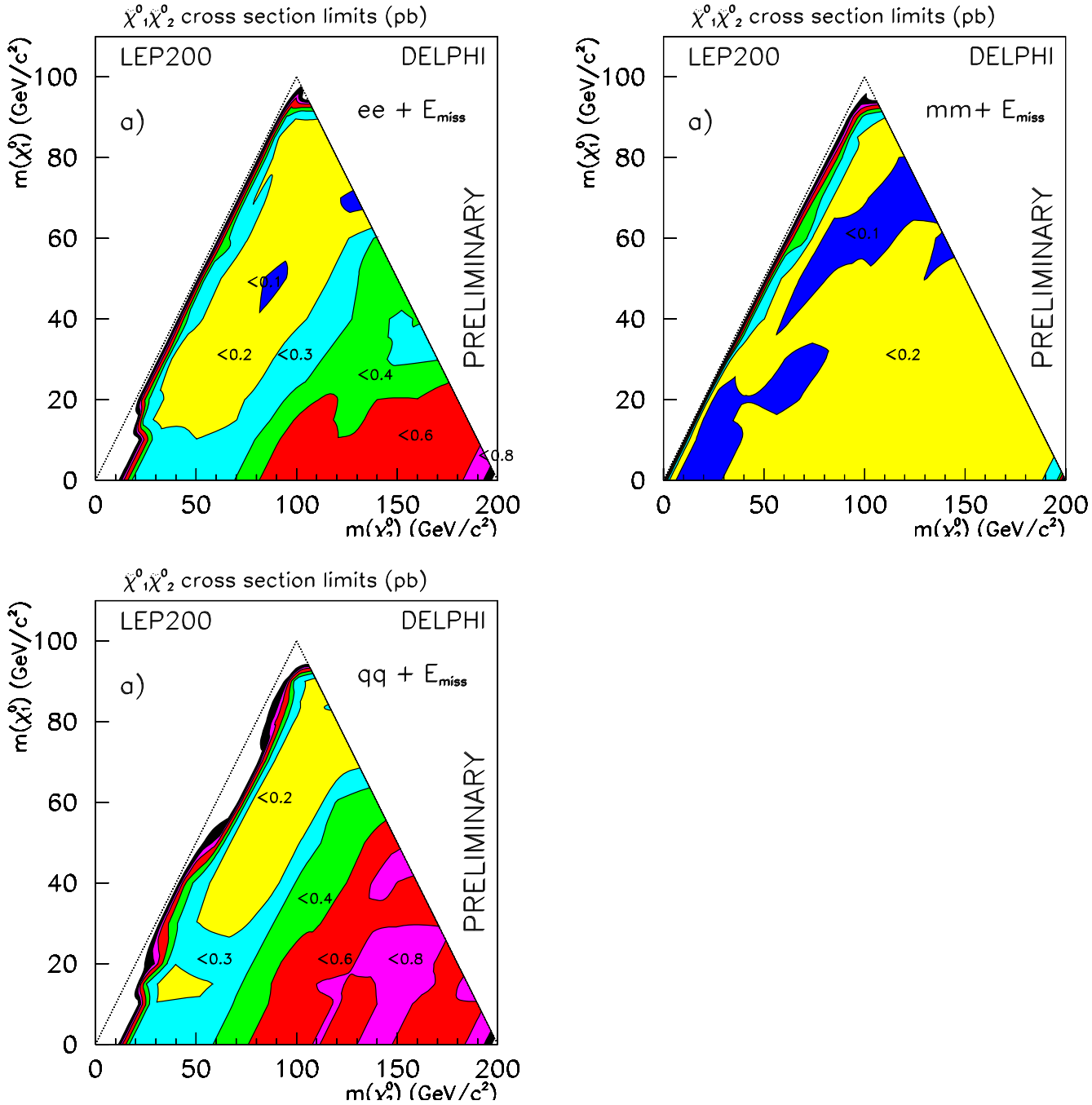

Figure 7: Upper limit on the cross–section times branching ractio for different neutralino search channel at 200 GeV

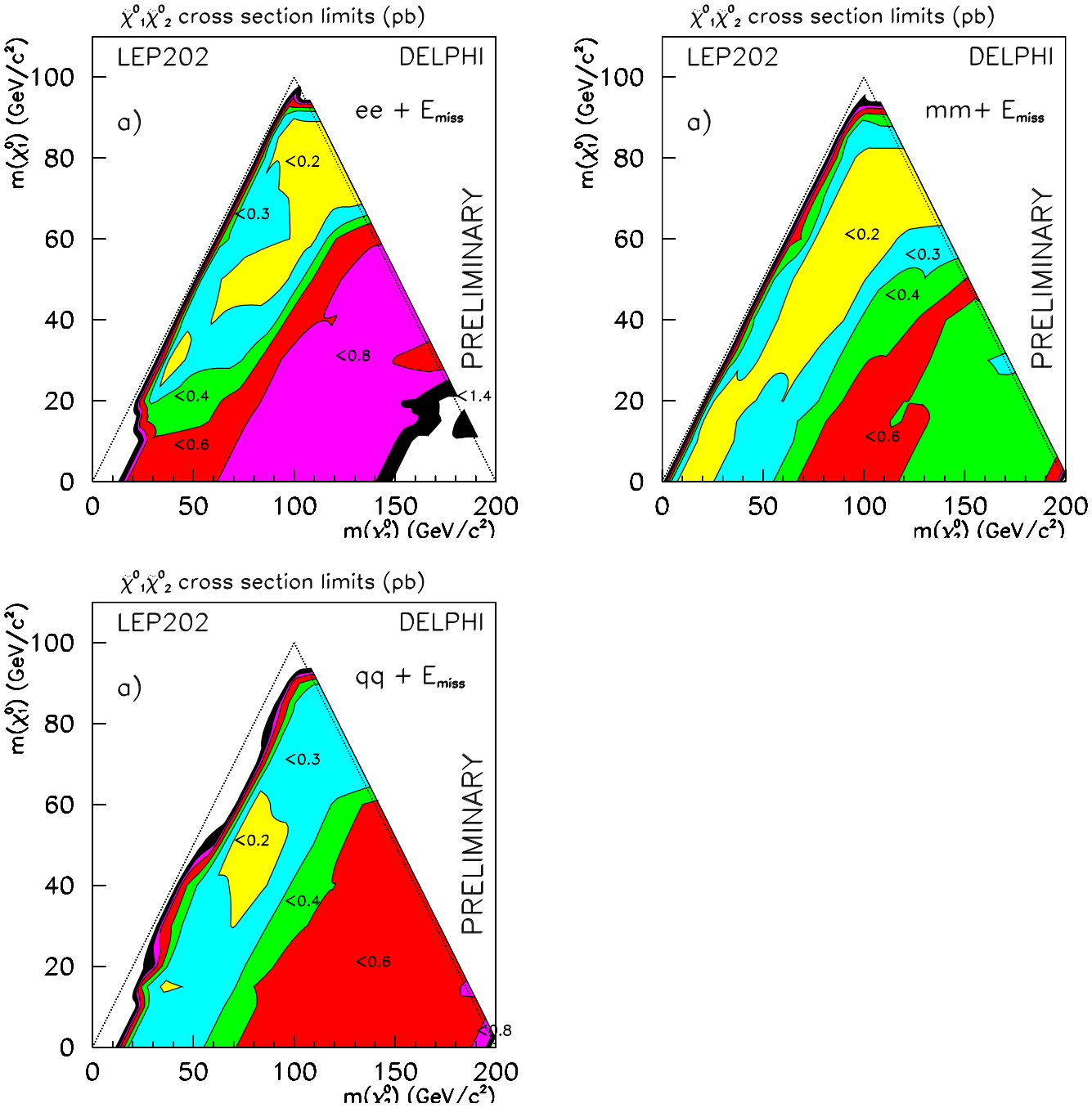

Figure 8: Upper limit on the cross–section times branching ractio for different neutralino search channel at 202 GeV